Decreased NKX3.1 Protein Expression in Focal Prostatic Atrophy, Prostatic Intraepithelial Neoplasia, and Adenocarcinoma: Association with Gleason Score and Chromosome 8p Deletion

Carlise R. Bethel,[1] Dennis Faith,[4] Xiang Li,[2] Bin Guan,[2] Jessica L. Hicks,[3] Fusheng Lan,[5] Robert B. Jenkins,[5] Charles J. Bieberich,[2] and Angelo M. De Marzo[3]

[1]Department of Biochemistry and Molecular Biology, Bloomberg School of Public Health; [2]Department of Biological Sciences, University of Maryland Baltimore County; [3]Departments of Pathology and Urology, The Sidney Kimmel Comprehensive Cancer Center at Johns Hopkins, The Johns Hopkins University School of Medicine, Baltimore, Maryland; [4]The University of Minnesota School of Medicine, Minneapolis, Minnesota; and [5]The Mayo Clinic, Rochester, Minnesota

Abstract

***NKX3.1* is a homeobox gene located at chromosome 8p21.2, and one copy is frequently deleted in prostate carcinoma. Prior studies of *NKX3.1* mRNA and protein in human prostate cancer and prostatic intraepithelial neoplasia (PIN) have been conflicting, and expression in focal prostate atrophy lesions has not been investigated. Immunohistochemical staining for NKX3.1 on human tissue microarrays was decreased in most focal atrophy and PIN lesions. In carcinoma, staining was inversely correlated with Gleason grade. Fluorescence *in situ* hybridization showed that no cases of atrophy had loss or gain of 8p, 8 centromere, or 8q24 (*C-MYC*) and only 12% of high-grade PIN lesions harbored loss of 8p. By contrast, NKX3.1 staining in carcinoma was correlated with 8p loss and allelic loss was inversely related to Gleason pattern. Quantitative reverse transcription-PCR for *NKX3.1* mRNA using microdissected atrophy revealed a concordance with protein in five of seven cases. In carcinoma, mRNA levels were decreased in 6 of 12 cases but mRNA levels correlated with protein levels in only 4 of 12 cases, indicating translational or post-translational control. In summary, NKX3.1 protein is reduced in focal atrophy and PIN but is not related to 8p allelic loss in these lesions. Therefore, whereas genetic disruption of *NKX3.1* in mice leads to PIN, nongenetic mechanisms reduce NKX3.1 protein levels early in human prostate carcinogenesis, which may facilitate both proliferation and DNA damage in atrophic and PIN cells. Monoallelic deletions on chromosome 8p are associated with more advanced invasive and aggressive disease.** (Cancer Res 2006; 66(22): 10683-90)

Introduction

Prostatic adenocarcinoma is one of the most common malignancies, representing the second leading cause of cancer death in American men (1). *NKX3.1* is located on chromosome 8p21.2 within a region that shows loss of heterozygosity (LOH) in prostate cancer in approximately 50% to 85% of cases (2, 3). Given that mutations in the remaining allele of *NKX3.1* have not been detected (4, 5), *NKX3.1* may function as a haploinsufficient tumor suppressor gene. That loss of one allele of *NKX3.1* occurs early in prostate carcinogenesis is evidenced by the finding that LOH on chromosome 8p has been reported to occur in high-grade prostatic intraepithelial neoplasia (PIN), a lesion that is a putative precursor to many invasive prostatic carcinomas (6), at a frequency between 20% and 80% (7–9).

Targeted disruption of *Nkx3.1* in mice results in abnormal prostate ductal morphogenesis and protein secretion (10–12). Although *Nkx3.1* homozygous mutant mice do not develop invasive carcinoma, epithelial hyperplasia and PIN lesions arise with age. Compound mutant mouse studies indicate that cooperativity exists between *Nkx3.1* and the tumor suppressors *Pten* and *Cdkn1b* (encoding p27; refs. 13–17). These compound mutants develop PIN lesions that progress to invasive carcinomas and at times to metastatic disease. Because the effects are seen in *NKX3.1* heterozygotes, haploinsufficiency of *Nkx3.1* also seems to play a role in tumor progression.

Several studies have analyzed NKX3.1 protein expression by immunohistochemistry in human prostate cancer specimens. In a study of PIN and carcinoma, loss of NKX3.1 protein staining was reported in ~20% of PIN lesions and ~40% of carcinomas, and loss of expression correlated with high Gleason score, advanced tumor stage, the presence of metastatic disease, and hormone-refractory disease (18). However, a more recent study reported that NKX3.1 protein was highly expressed in adenocarcinoma, irrespective of tumor grade (19). Asatiani et al. (20) revisited the question of NKX3.1 protein expression in prostate cancer and reported that complete loss of staining was very rare (~5% of cases) but that the intensity of staining in carcinoma was reduced compared with normal epithelium. The reduction of intensity correlated with the combination of loss of one copy of *NKX3.1* and hypermethylation of cytosine residues in specific CpG dinucleotides near the putative *NKX3.1* promoter region as well as with Gleason grade. Thus, when examining the body of data as a whole, there is still substantial controversy about NKX3.1 protein expression in human prostate cancer.

In terms of *NKX3.1* mRNA expression levels in human prostate tumors, there have also been conflicting results. Semiquantitative reverse transcription-PCR (RT-PCR) analyses of benign and malignant tissues revealed overexpression of *NKX3.1* mRNA in 31% of cancer specimens, decreased expression in 21%, and no change in 48% (21). In the study by Xu et al. (21), overexpression of

Note: Supplementary data for this article are available at Cancer Research Online (http://cancerres.aacrjournals.org/).

Requests for reprints: Angelo M. De Marzo, Departments of Pathology and Urology, The Sidney Kimmel Comprehensive Cancer Center at Johns Hopkins, The Johns Hopkins University School of Medicine, Bunting-Blaustein Cancer Research Building, Room 153, 1650 Orleans Street, Baltimore, MD 21231. Phone: 410-614-5686; Fax: 410-502-9817; E-mail: ademarz@jhmi.edu.

doi:10.1158/0008-5472.CAN-06-0963

NKX3.1 mRNA correlated with metastatic disease. In contrast, other groups have reported *NKX3.1* mRNA to be similarly expressed in normal prostate and tumors of various grades (5, 19), and this correlated with NKX3.1 protein (19, 20). Thus, controversy remains about *NKX3.1* mRNA expression in human prostate cancer.

Focal prostatic atrophy is a common finding in older men and encompasses several morphologic variants (22). Some of these lesions are proposed as potential precursors to prostate cancer based on their frequent occurrence in proximity to carcinoma (23–26) and molecular alterations (see below). Focal prostate atrophy commonly merges directly with low- and high-grade PIN (24, 25, 27), suggesting that some PIN lesions arise directly from atrophy. More rarely, focal atrophy seems to merge directly with small carcinoma lesions (23, 27–29). Two common types of focal prostatic atrophy, simple atrophy and postatrophic hyperplasia (PAH), are often highly proliferative and associated with inflammation (24, 30) and are referred to as proliferative inflammatory atrophy (PIA).[6]

We have proposed a multistep progression model that leads from normal epithelium to focal prostatic atrophy to PIN and then to carcinoma (24, 31). In this model, ongoing injury to the prostate epithelium, as a result of inflammation and/or dietary exposures, results in cell damage and cell death. Cell regeneration ensues and this is manifest morphologically as PA. These atrophic cells are presumed to be responding to increased oxidative and/or nitrosative stress (32–34) and are apparently undergoing tissue repair/renewal (35, 36). Many of the atrophic cells possess a phenotype intermediate between basal cells and mature luminal cells (33, 36). These cells may then undergo somatic genome alterations, including methylation of the *GSTP1* promoter and telomere shortening, leading to neoplastic transformation. There have been no reports, however, in which NKX3.1 protein expression in focal prostate atrophy has been examined. *NKX3.1* mRNA expression in prostatic atrophy has only been briefly described as being decreased relative to normal (5).

The primary objective of this study was to determine the potential relevance of molecular alterations of NKX3.1 in relation to our progression model of human prostate carcinogenesis. We now report the results of the following: (*a*) a quantitative analysis of the expression of NKX3.1 protein using a novel anti-NKX3.1 polyclonal antibody on tissue microarrays (TMA) containing matched samples of normal, focal prostate atrophy, PIN, and clinically localized adenocarcinoma of various Gleason grades; (*b*) a study to correlate NKX3.1 protein levels with chromosomal alterations on chromosome 8 using fluorescence *in situ* hybridization (FISH) on the same TMA specimens; and (*c*) a study to determine if NKX3.1 protein levels correlate with mRNA levels using laser capture microdissection of frozen tissue specimens for quantitative RT-PCR.

Materials and Methods

Generation of anti-NKX3.1 rabbit polyclonal antibodies. To derive polyclonal anti-NKX3.1 antibodies, a His-tagged polypeptide containing the NH_2-terminal 153 amino acids of human NKX3.1 was expressed in *Escherichia coli* and purified over a nickel affinity resin followed by anion exchange chromatography. Fractions with >95% pure His-tagged NH_2-terminal NKX3.1 were used to immunize rabbits. Immunoglobulins from production bleeds were purified using a protein A column.

Tissues and TMA construction. This study was approved by our institutional internal review board. Tissue specimens were obtained from radical retropubic prostatectomies done at the Johns Hopkins Hospital (Baltimore, MD). Patient ages ranged from 44 to 74 years. Final Gleason sums varied from 5 to 9, with pathologic stages of the tumors ranging from T2N0Mx to T3BN1Mx (Supplementary Table S1).

For NKX3.1 immunostaining, we used five high-density TMAs. Two of these were designed to compare matched normal and atrophy, and the other three were designed to compare matched normal and carcinoma. One of the atrophy arrays consisted of matched normal (n = 4 cores each from 20 patients) and atrophy (n = 4 cores each from 3 separate atrophy lesions per patient for a total of 58 different atrophy lesions from the 20 patients). For the second atrophy array, there were four cores of normal and four cores of atrophy each from 39 patients. The classification of prostate atrophy lesions was according to De Marzo et al. (22). Several TMA cores incidentally contained PIN. For the matched cancer and normal TMAs, the arrays were constructed with matched samples from 40 patients per array as described previously (34, 37). Images of each TMA core were captured by scanning of the TMA slides using the Automated Cellular Imaging System II (ACIS II) from Clarient, Inc. (Aliso Viejo, CA) and were imported into the TMAJ Images application[7] as described (37). Histologic diagnoses were applied to all images used for the analyses, and these diagnoses are listed in Supplementary Table S2.

Immunohistochemistry. Immunohistochemistry was done with the EnVision+ kit (DakoCytomation, Carpinteria, CA). Slides were steamed for 20 minutes in 10 mmol/L citrate buffer (pH 6.0) for antigen retrieval. Slides were incubated with primary antibodies (1:5,000 dilution) overnight at 4°C. For keratin 8 (CK8) staining, slides were prepared as described above and stained with CK8 antibody (1:800 dilution; InnoGenex, San Ramon, CA) at room temperature for 45 minutes.

Evaluation of immunohistochemical staining. The average intensity and area of staining were analyzed on TMA slides using the ACIS II (37). Tissue cores containing more than one type of tissue (i.e., atrophy and carcinoma) were not used for data analysis. The area of nuclear staining for NKX3.1, which is epithelial specific, was normalized to the area of keratin 8 staining of the cytoplasm as described (37). Statistical analyses were done using Stata 8.0 software (Stata, College Station, TX).

For each TMA core, a mean intensity of staining and an area of staining were assigned by the ACIS. In most cases, there were multiple cores from the same patient showing the same diagnosis, and image analysis values were averaged for statistical analysis.

Fluorescence *in situ* hybridization. The FISH technique was modified from that described previously (38). FISH hybridization was done with the multicolor probes (ProVysion, Vysis, Inc., Downers Grove, IL) to detect and quantify chromosome 8 centromere probe [chromosome enumeration probe 8 (CEP8)] and with two locus-specific probes, the lipoprotein lipase (LPL; 8p21.3) and the c-MYC 8q24 probe. Three of the same TMAs used for NKX3.1 staining were used for FISH, and three additional TMAs were also used for FISH from which FISH data from additional PIN lesions were obtained. Up to 30 nonoverlapping interphase nuclei from each core/region of benign normal-appearing epithelium, atrophy, PIN, and carcinoma were counted for each probe. For each TMA core that was counted by FISH, there was an internet-based image of a H&E-stained adjacent TMA section that was annotated with the pathologist's diagnosis. Normal value studies using prostate tissue have been previously reported (38). An inspection of the copy number of each FISH signal in a nucleus was recorded, and the ratios and distributions of each probe (LPL, c-MYC, and CEP8) of a given core were categorized as normal, gain, abnormal increase, or loss. The threshold values for these categories were chosen to minimize the detection of false-positive changes. The normal category required <30% of epithelial

[6] For similar lesions without inflammation, the term proliferative atrophy (PA) may be used. In this article, most of the lesions examined represent simple atrophy and PAH. Therefore, we use the terms focal prostate atrophy and PIA/PA interchangeably.

[7] See http://tmaj.pathology.jhmi.edu.

nuclei with three or more signals and <60% of epithelial nuclei with zero or one signal for an applied probe. The gain category required ≥30% of epithelial nuclei with three or more signals for an applied probe. The category of abnormal increase of c-MYC (8p24) required ≥30% of epithelial nuclei with three or more signals for c-MYC (8p24) and an overall 8p24/CEP8 ratio of >1.30. The category of loss of CEP8 required ≥60% of epithelial nuclei with zero or one signal for CEP8. The category of loss of 8p required ≥60% of epithelial nuclei with zero or one signal for LPL and the overall LPL/CEP8 ratio of <0.80.

Laser capture microdissection. For each case, two serial 7-μm frozen sections were fixed in 70% ethanol for 1 minute followed by a rinse in diethyl pyrocarbonate–treated water for 30 seconds. Slides were lightly stained with hematoxylin for 45 seconds and dehydrated. Regions of normal epithelium, atrophy, and tumor were microdissected using the AutoPix Automated Laser Capture Microdissection System (Arcturus Engineering, Inc., Mountain View, CA). Immunohistochemistry was also done to compare NKX3.1 staining in regions microdissected for quantitative RT-PCR.

Quantitative RT-PCR. Total RNA was isolated from laser capture microdissected cells with the Absolutely RNA Microprep RNA Isolation kit (Stratagene, La Jolla, CA) following the manufacturer's protocol. On-column DNase I digestion was done during the RNA extraction. RNA was ethanol precipitated and used to generate cDNA with the iScript cDNA Synthesis kit (Bio-Rad, Richmond, CA). Quantitative PCR was done using SYBR Green I and the iCycler (Bio-Rad) with intron-spanning primers for NKX3.1 (5′-GAATCCGTATGCCCCGCTG-AATCT-3′ and 5′-ACCCTTGCCAGTGCGT-GTGC-3′) and for TATA-binding protein (TBP; 5′-CACGAACCACGGCACT-GATT-3′ and 5′-TTTTCTTGCTGCCAGTCTGGAC-3′). For quantification of *NKX3.1* mRNA levels, we normalized to *TBP* mRNA, which was used as an endogenous control. The relative amount of *NKX3.1* mRNA in each experimental sample was determined using the $\Delta\Delta C_t$ method (39). Two independent triplicate quantitative PCR experiments were done for each case.

Results

Visual/qualitative assessment of NKX3.1 immunostaining. The specificity of the newly generated polyclonal antibody is shown as supplementary data (Supplementary Fig. S1). In normal epithelium, NKX3.1 staining was intense in the nuclei of most secretory luminal cells (Fig. 1*A* and *B*), with very faint or negative cytoplasmic staining. The pattern of nuclear staining, as seen at high power, was granular, with both fine granules and more clumped granules seen. Luminal cells throughout a given prostate acinus did show some variability in the intensity of nuclear staining. Although many acini showed negative staining in basal cells, many acini contained weak staining in the nuclei of basal cells (Figs. 1*B* and 3*A*). There was no staining in nonepithelial tissues in the prostate.

Compared with normal epithelium, most atrophy lesions contained reduced NKX3.1 protein (Fig. 1*C* and *D*). Both the intensity of staining and the percentage of cells staining were decreased albeit to a variable extent. Often, the entire lesion was reduced, but in other cases only part of the lesion, or even individual acini, showed reduced staining. At times, some cells in atrophy showed strong staining that was similar to normal epithelium (Fig. 1*D, arrowhead*). The granular pattern of nuclear staining in atrophy was similar to that seen in normal-appearing epithelium as was the general lack of cytoplasmic staining.

NKX3.1 immunostaining was seen in all cases of PIN, but the intensity in most cells was usually less than in the normal-appearing luminal cells (Fig. 2*B*), and there were a variable number of cells in the luminal compartment with very faint nuclear staining. Cytoplasmic staining in PIN was generally similar to that in normal epithelium, although at times it was somewhat more prominent in PIN than in normal.

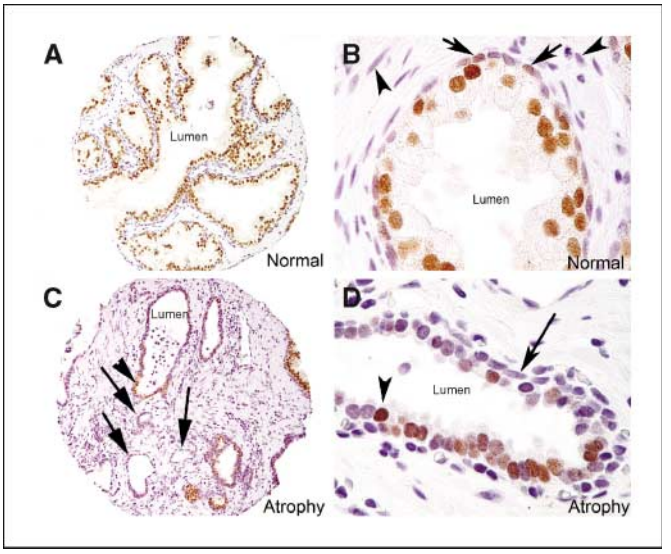

Figure 1. Immunohistochemical staining for NKX3.1 in normal and atrophy. *A,* low-power view of normal-appearing epithelium. Magnification, ×100. Note strong staining in luminal cells and negative staining in stroma. *B,* high-power view of region in part (*A*) showing weak staining in some basal cells (*arrows*) and negative staining in stromal cells (*arrowheads*). Magnification, ×600. *C,* reduced staining seen in a simple atrophy lesion from the same patient as that in (*A*). Magnification, ×100. *D,* high-power view of another simple atrophy lesion showing reduced but variable staining. *Arrow,* negatively staining basal cells. Note many luminal cells are weak or negative. *Arrowhead,* strongly staining luminal cell. Magnification, ×600.

Most carcinomas showed reduced, albeit variable, staining for NKX3.1 (Fig. 3*B* and *F*). Many carcinomas showed very mild reductions in intensity of staining, with occasional increases in the number of entirely negatively staining cells. Others showed a more marked reduction in intensity in many of the cells, with more cells staining completely negatively (Fig. 3*F*). In rare cases, mitotic figures were seen, and these cells were clearly negative for NKX3.1 staining (data not shown). Cytoplasmic staining in cancer was generally similar to that seen in normal epithelium, although like PIN there were several cases with slightly stronger cytoplasmic staining than that seen in normal-appearing epithelium.

Quantitative image analysis of NKX3.1 staining. Automated image analysis[8] showed that, compared with normal epithelium, the intensity of staining in atrophy lesions was reduced significantly (Fig. 4*A*). The area of nuclear staining in atrophy compared with normal epithelium was even more reduced than the intensity values (Fig. 4*C*; Table 1). There was no difference in intensity or area of NKX3.1 staining when stratified by type of atrophy (e.g., simple atrophy versus PAH versus simple atrophy with cyst formation; data not shown).

The intensity of NKX3.1 staining in PIN lesions was also reduced significantly in >75% of lesions when compared with normal-appearing epithelium (Fig. 4*B*; Table 1). PIN lesions also showed a reduction in area of staining, yet this reduction was not statistically significant (Table 1B).

In carcinoma, the intensity of NKX3.1 staining was significantly reduced compared with normal, and similar to PIN lesions, the area of staining in carcinoma was reduced but this difference was not significant (Table 1). In terms of tumor grade, we analyzed the

[8] Only nuclear staining was evaluated for image analysis.

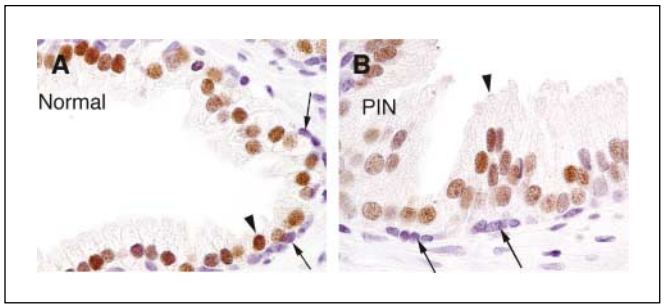

Figure 2. Immunohistochemical staining for NKX3.1 in normal and PIN. *A,* high-power view of staining in normal-appearing epithelium. Magnification, ×600. *B,* high-power view of staining in high-grade PIN from the same patient as in (*A*). *Arrowhead,* luminal cell; *arrows,* basal cells that are staining negatively. Magnification, ×600.

intensity and area of staining for NKX3.1 in the TMA spots in relation to the Gleason score for the prostatectomy case. The intensity for NKX3.1 staining was decreased in all Gleason scores represented; however, the decrease was greater in higher-grade tumors (Gleason scores 8-9; Table 1; Fig. 4*B*). In terms of area of staining in carcinoma, there was a significant reduction compared with normal only in cases with higher-grade tumors (Gleason sum 8-9; Fig. 4*D*; Table 1). When the data were analyzed by Gleason pattern of the individual tissue cores, similar results were obtained—those spots with higher grade were generally found to have less intense NKX3.1 staining and less area of staining (data not shown). In multivariate regression analysis, including both Gleason score and NKX3.1 area of staining, only Gleason score remained significant at predicting pathologic stage (data not shown).

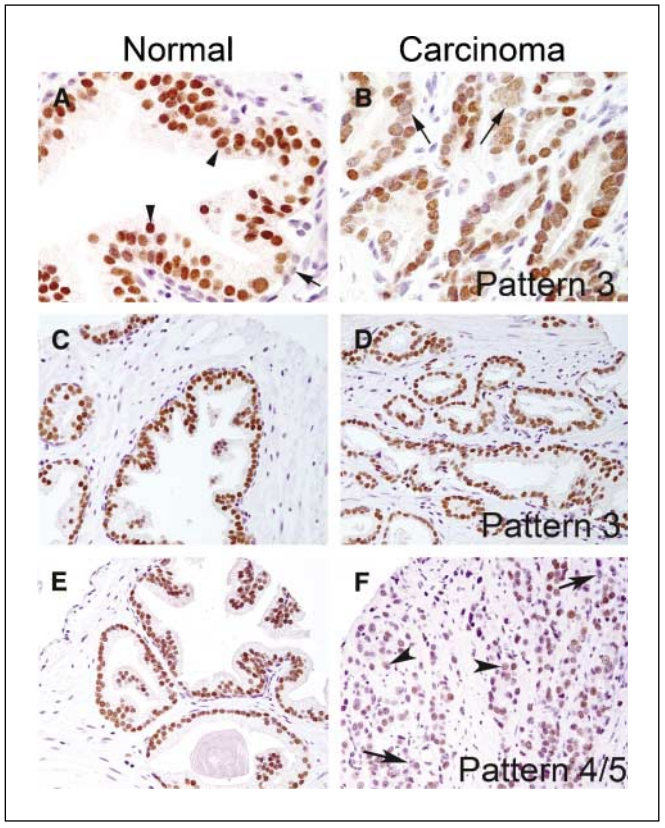

Figure 3. Immunohistochemical staining for NKX3.1 in normal and carcinoma. *A, C,* and *E,* normal-appearing epithelium. Magnifications, ×400 (*A*), ×200 (*C*), and ×200 (*E*). *A, arrowheads,* luminal cells; *arrow,* basal cell staining weakly. *B, D,* and *F,* carcinoma lesions matched to those cases from (*A*), (*C*), and (*E*), respectively, shown at the same magnification as the matched pair. *B,* Gleason pattern 3, mild to moderate reduction in intensity with little reduction in area of staining. *Arrows,* weakly staining tumor cells. *D,* Gleason pattern 3, very mild reduction in intensity with no reduction in area of staining. *F,* Gleason pattern 5, marked reduction in intensity and area of staining. *Arrowheads,* weakly staining tumor cells; *arrows,* negatively staining tumor cells.

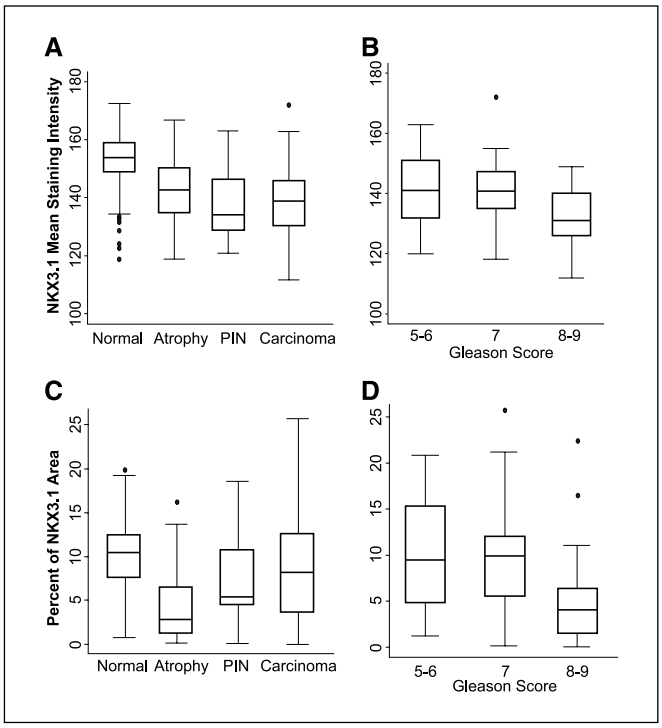

Figure 4. Automated image analysis of NKX3.1 staining in normal and lesional tissues. *Box plots,* distribution of staining intensity (*A* and *B*) or areas (*C* and *D*) of the average values of the different tissue types. *B* and *D, X axis,* Gleason scores for the radical prostatectomy specimens. *Boxes,* 25th and 75th percentile with the median (*line inside the box*). *Whiskers,* adjacent values; *filled circles,* outliers.

Because *NKX3.1* is a tumor suppressor with known inhibitory effects on cell proliferation (13, 40), we determined whether cells in atrophy that were proliferating, as assessed by Ki67 staining, contained lower levels of NKX3.1. Double-label immunofluorescence was done on one TMA containing atrophy and matched normal and one containing carcinoma and matched normal. By immunofluorescence, there were clear gradations in staining for both makers (Supplementary Fig. S2). In general, when a cell was positive for any amount of Ki67, it tended to be negative or only weakly positive, for NKX3.1, compared with other cells in the same lesions (Supplementary Fig. S2). In cells with the most Ki67 staining, NKX3.1 was virtually always negative. This inverse relation between Ki67 and NKX3.1 suggests that NKX3.1 protein is regulated in a cell cycle–dependent manner.

NKX3.1 mRNA expression. To evaluate the levels of *NKX3.1* mRNA, quantitative real-time PCR using RNA prepared from laser microdissected frozen tissue sections was done. Eight atrophy lesions and matched normal-appearing tissues were evaluated. Adjacent sections were also immunostained with the anti-NKX3.1

antibody (in seven of the cases). Three of eight of the atrophy cases microdissected showed a decrease in relative *NKX3.1* mRNA abundance (cases A, G, and J; Table 2). In the two of these three cases (cases A and G), immunohistochemical analysis revealed that the protein levels were also reduced. Five cases of atrophy displayed no change or increased *NKX3.1* mRNA levels compared with matched normal specimens (cases C, D, E, F, and H), yet two had reduced protein levels (40%; cases E and F). There were no cases of atrophy where the mRNA was decreased but the protein staining was intact. Overall, therefore, mRNA and protein levels in focal prostate atrophy lesions were concordant in five of seven cases that were evaluated (Table 2). The two cases that were not concordant showed that, despite normal mRNA levels, protein staining was decreased.

In carcinoma, the *NKX3.1* mRNA was reduced in 6 of 12 cases, was normal in 5 cases, and was increased in 1 case (Table 2). Of the six cases with reduced mRNA that were stained by immunohistochemistry, two (33%; cases D and F) showed reduced protein staining. Of the six cases with normal or elevated mRNA levels, however, four of these also showed reduced protein staining (66%; cases I, K, L, and N). There were three cases of carcinoma in which the mRNA levels were reduced, yet the protein staining seemed intact. Overall, therefore, only four of nine cases of carcinoma that could be evaluated were concordant between mRNA and protein.

Relation of NKX3.1 protein and chromosome 8p deletion. Three of the same TMAs used above were subjected to FISH. Two of the TMAs consisted of matched atrophy and normal-appearing epithelium and the other was from matched normal and adenocarcinoma. A total of 466 TMA spots from 33 patients were analyzed, including 359 cores of normal and 245 cores of atrophy. Although one atrophy and one normal TMA core were close to the cutoff for deletion of 8p, none of the normal or atrophic regions were found to meet our strict criteria for loss or gain of 8p, 8 centromere, or *C-MYC*. As in previous studies, (26, 41), we also compared the fraction of cells with three or more chromosome 8 centromere signals in atrophy and matched normal in one of the TMAs. Although there was a significant increase in the fraction of cells in atrophy that harbored three or more signals for chromosome 8 centromere compared with normal (2.4% for atrophy versus 1.2%; $P = 0.024$, Wilcoxon rank sum), no TMA cores containing prostate atrophy were considered to have gained chromosome 8 centromere in a clonal fashion.

In carcinoma, deletion of 8p sequences occurred in 52% of TMA cores and much more frequently in those that were poorly differentiated (74% for Gleason patterns 4-5) compared with those cores that were more well differentiated (33% for Gleason pattern 3; Supplementary Table S4). This increase in the fraction of high-grade lesions with 8p deletion is consistent with other previous studies (42–44). In addition, both reduced intensity and reduced area of NKX3.1 staining correlated with LOH (Fig. 5; $P < 0.001$ for area and intensity, Kruskal-Wallis).

On these three TMAs, there were six high-grade and two low-grade PIN lesions. Of these, there was one deletion of one allele on 8p in a high-grade lesion (one of six, 17%) and no gains or losses

Table 1.

A. Statistical analysis of NKX3.1 staining intensity and area by image analysis using paired samples

	Normal	Atrophy	PIN	Carcinoma
Intensity				
Normal	—	<0.0001 (n = 71)	0.0064 (n = 15)	<0.0001 (n = 111)
Atrophy			0.4496 (n = 11)	0.0198 (n = 56)
PIN				0.9 (n = 14)
Carcinoma				—
Area				
Normal	—	<0.0001	0.3635	0.1
Atrophy			0.0409	<0.0001
PIN				0.1981
Carcinoma				—

B. Statistical analysis of NKX3.1 staining by image analysis in relation to Gleason score

Gleason score	5-6	7	8-9
NKX3.1 mean intensity			
Normal	<0.0001 (n = 53)	0.0002 (n = 33)	<0.0001 (n = 24)
NKX3.1 mean area			
Normal	0.9823	0.9644	0.0043

NOTE: First numbers are *P*s. n represents the number of matched pairs of samples for the indicated comparisons. The n values for area are the same as for intensity. For intensity, atrophy, PIN, and carcinoma are less than normal, and atrophy is greater than carcinoma. For area, atrophy is less than normal, PIN, and carcinoma. All *P*s were obtained from the Wilcoxon matched pairs signed-rank test. Comparisons are from the means of all cores from a given case with a given diagnosis. Gleason scores are from the radical prostatectomy specimen.

Table 2. Relative mRNA expression of NKX3.1 in prostate tissues

Case letter	Tissue	RNA	RNA down	Protein down	Grade	Stage	Concordant
A	Atrophy	0.5	+	+	7	T3AN0MX	+
C	Atrophy	5	−	−	7	T3AN0MX	+*
D	Atrophy	0.9	−	−	7	T3BN0MX	+
E	Atrophy	1.2	−	+	6	T2N0MX	−
F	Atrophy	1.5	−	+	8	T3AN1MX	−
G	Atrophy	0.3	+	+	6	T2N0MX	+
H	Atrophy	1	−	−	9	T3AN0MX	+
J	Atrophy	0.3	+	ND	7	T2XN0MX	ND
A	Tumor	0.3	+	−	7	T3AN0MX	−
B	Tumor	0.65	+	−	6	T2N0MX	−
C	Tumor	0.5	+	ND	7	T3AN0MX	ND
D	Tumor	0.3	+	+	7	T3BN0MX	+
E	Tumor	1.1	−	−	6	T2N0MX	+
F	Tumor	0.5	+	+	8	T3AN1MX	+
H	Tumor	0.3	+	−	9	T3AN0MX	−
I	Tumor	2.8	−	+	9	T3AN0MX	−
K	Tumor	0.9	−	+	9	T3BN0MX	−
L	Tumor	0.9	−	+	9	T3AN0MX	−
M	Tumor	1	−	−	9	T3BN0MX	+
N	Tumor	1.1	−	+	7	T2N0MX	−

NOTE: "RNA" is expressed as quantity relative to matched normal epithelium from the same case. Grade and stage indicate values determined at radical prostatectomy. Case letter indicates which patient the sample was from. All cases had matched normal-appearing epithelium, and the mRNA value for the normal was set to 1.
Abbreviation: ND, not determined.
*RNA was elevated above normal with normal protein staining.

of 8 centromere or 8q24 in any of the PIN lesions. Three additional TMAs containing matched cancer and normal prostate were evaluated and these contained 19 high-grade PIN lesions and 8 low-grade PIN lesions and none of these had gain of 8 centromere or 8q24. Of these, there were two cases with deletion of one allele on 8p in two of the high-grade lesions and none in the low-grade PIN. Thus, overall, 3 of 25 (12%) high-grade and 0 of 10 (0%) low-grade PIN lesions had loss of 8p.

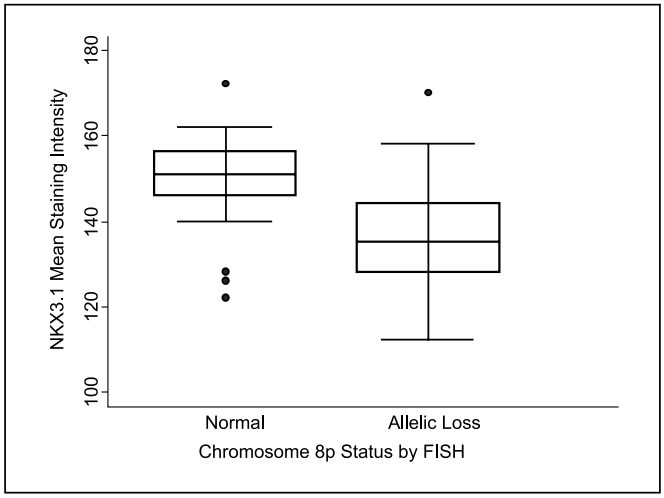

Figure 5. Box plot of distribution of NKX3.1 staining intensity values as a function of chromosome 8p allelic status.

Discussion

Immunohistochemical analyses of atrophy showed a profound decrease in both staining intensity and percentage area of staining for NKX3.1. These observations fit well with the known functions of NKX3.1 in growth control and with a multistep progression model that leads from normal epithelium to PIA to PIN and then to carcinoma (24, 31). The diminished expression of NKX3.1 observed in PIA may reflect a response to oxidative stress. By contrast, because lack of NKX3.1 results in increased oxidative DNA damage by controlling expression of antioxidant enzymes (45), reduced NKX3.1 in PIA may contribute to increased oxidant damage in these lesions.

The decreased level of NKX3.1 in PIA may reflect the intermediate cell phenotype that we have proposed for many atrophic luminal cells in PIA (36). The levels in most cells that were positive were greater than that seen in basal cells but less than that seen in mature columnar luminal cells. The intermediate level of androgen receptor in PIA (24) and the androgen responsiveness of NKX3.1 fit well with this model.

The molecular basis of diminished NKX3.1 in PIA is not clear. Allelic loss does not seem to play a role because many of the atrophic lesions had reduced NKX3.1 protein but none had deletion on chromosome 8p21.3 in the region of the LPL probe. It is still possible, albeit unlikely, that there are small deletions of chromosome 8p21.2 in the *NKX3.1* locus itself that would not be detected by the LPL probe. Additional studies using more refined FISH probes will be necessary to rule this out. Quantitative analyses of *NKX3.1* steady-state mRNA levels revealed concordance in five of seven cases examined between *NKX3.1* mRNA and protein levels in PIA, suggesting that control of NKX3.1 protein levels in

prostate atrophy is related to mRNA levels in most cases. These results agree with Ornstein et al. (5), who examined *NKX3.1* mRNA levels in frozen prostate tissues by *in situ* hybridization with a radiolabeled probe and reported decreased signal in "atrophic" regions, albeit the number of cases with atrophy was not indicated. The data are consistent with regulation of *NKX3.1* mRNA in atrophy at the level of transcription, mRNA processing, or mRNA stability. In two cases, mRNA was normal and protein was decreased. Thus, regulation of NKX3.1 protein levels likely occurs at multiple steps, including at the level of translation and/or protein stability. The serine-threonine kinase CK2 has recently been shown to play a central role in the stability of NKX3.1 by protecting it from proteasomal degradation (46).

It is not clear precisely why there are increased signals for chromosome 8 centromere in PIA. One potential explanation is that because the fraction of cells is still very low compared with cases that show gain in a clonal fashion (i.e., >30% of cells have three or more signals), it is possible that this finding simply reflects the known increase in proliferative fraction in prostate atrophy compared with normal epithelium. Cells that have traversed into late S phase or G_2-M would have double the number of chromosomes and thus would be expected to show an increase in centromeric FISH signals. In the single previous study that mentioned prostate atrophy using FISH for chromosome 8p, two of seven prostate atrophy lesions had allelic loss (41). The most likely explanation for our lack of finding LOH on 8p in atrophy is that we used a more stringent statistical cutoff to indicate loss of the 8p probe (41).

NKX3.1 staining intensity was significantly diminished (P = 0.0064) in PIN lesions compared with normal epithelium, in agreement with a recent study (20). In this study, we report the novel finding that reduced NKX3.1 protein expression in PIN does not correlate with loss of chromosome 8p because most PIN (>75%) lesions showed decreased protein expression but only 12% showed loss of 8p. Thus, loss of NKX3.1 protein seems to precede genetic loss in prostate neoplasia. These data help to clarify the temporal ordering of molecular alterations in human prostate carcinogenesis and indicate that additional mechanisms of down-regulation of NKX3.1, other than gene deletion, are important in human PIN.

Our study revealed a statistically significant reduction in NKX3.1 immunostaining in prostate cancer compared with normal epithelium, in agreement with several previous reports (18, 20). The studies reported here showed a clear correlation between reduced NKX3.1 protein expression and high Gleason grade, which also agrees with recent study by Asatiani (20).

Unlike what we observed in most PIA lesions, a general lack of concordance between the mRNA and protein accumulation in carcinoma was found. In some tumors, both mRNA and protein were diminished to a similar extent, in agreement with a recent report (19). In others, however, reduced protein accumulation was observed in lesions with a normal mRNA level. A third class of lesions showed reduced NKX3.1 staining despite having a greater-than-normal level of mRNA. Increased *NKX3.1* mRNA levels have been previously reported in a subset of cases (21). The most likely scenario is that multiple mechanisms operate to down-regulate NKX3.1 protein in normal, atrophic, and neoplastic prostate epithelial cells.

One mechanism of NKX3.1 regulation is at the level of gene dosage. Our data show a strong correlation between 8p loss and NKX3.1 level in carcinoma but not in atrophy or PIN. This suggests that loss of one *NKX3.1* allele may be sufficient to result in a measurable decrease in protein accumulation that may result in a state permissive for cell cycle progression. This correlation seen in our study in carcinoma agrees with a recent study that analyzed cases with 8p21 loss (20). Although, in that study, the authors also reported that the methylation status of individual CpG dinucleotides in sequences upstream of the transcription start site, when combined with loss of 8p sequences, was the best predictor of decreased protein levels. However, there is currently no functional evidence linking the putative sites of methylation to the transcriptional control of *NKX3.1*. An enhancer-containing region well downstream of the mouse *NKX3.1* gene has recently been reported to be necessary and sufficient for prostate-restricted gene expression *in vivo* (47). It will be important to examine the methylation status of its cognate in the human *NKX3.1* locus.

In summary, we report that NKX3.1 protein is decreased in PIA/PA in the human prostate. In most cases, this relates to steady-state mRNA levels but does not relate to gene dosage. In PIN lesions, NKX3.1 was reduced but this too did not correlate with loss of chromosome 8p sequences. Indeed, only 12% of high-grade PIN lesions, and no low-grade PIN lesions, showed 8p21.3 loss by FISH, which is a lower value than even the lowest (20%) that has been reported previously. By contrast, 33% of Gleason pattern 3 and 74% of Gleason pattern 4/5 carcinomas contained 8p deletions, and the deletions correlated with NKX3.1 protein in carcinoma. Thus, deletion of sequences on chromosome 8p21.3 may be involved more with progression of invasive disease than in initiation of disease. Because NKX3.1 may protect cells from oxidative stress, these results support a model whereby low levels of NKX3.1 facilitate both proliferation and DNA damage in atrophic prostate epithelial cells and in PIN cells, increasing the risk of carcinogenesis. By the same mechanisms, reduced NKX3.1 in carcinoma may facilitate disease progression.

Acknowledgments

Received 3/14/2006; revised 6/19/2006; accepted 9/20/2006.

Grant support: National Cancer Institute (NCI) National Research Service Award grant CA94818-04 (C.R. Bethel), Public Health Services NIH/NCI grant R01CA84997 and NIH/NCI Specialized Program of Research Excellence in Prostate Cancer grant P50CA58236 (Johns Hopkins), and The Donald and Susan Sturm Foundation (A.M. De Marzo); NIH/NIDDK grant R01DK54067 and DAMD-03-1-0091 from the Congressionally Directed Medical Research Program (C.J. Bieberich).

The costs of publication of this article were defrayed in part by the payment of page charges. This article must therefore be hereby marked *advertisement* in accordance with 18 U.S.C. Section 1734 solely to indicate this fact.

We thank Dr. Alan K. Meeker for thoughtful discussions and the Johns Hopkins Brady Urological Institute Prostate Specimen Repository for prostate TMAs.

References

1. Jemal A, Murray T, Ward E, et al. Cancer statistics, 2005. CA Cancer J Clin 2005;55:10–30.
2. Sakr WA, Macoska JA, Benson P, et al. Allelic loss in locally metastatic, multisampled prostate cancer. Cancer Res 1994;54:3273–7.
3. Vocke CD, Pozzatti RO, Bostwick DG, et al. Analysis of 99 microdissected prostate carcinomas reveals a high frequency of allelic loss on chromosome 8p12-21. Cancer Res 1996;56:2411–6.
4. Voeller HJ, Augustus M, Madike V, Bova GS, Carter KC, Gelmann EP. Coding region of NKX3.1, a prostate-specific homeobox gene on 8p21, is not mutated in human prostate cancers. Cancer Res 1997;57:4455–9.
5. Ornstein DK, Cinquanta M, Weiler S, et al. Expression studies and mutational analysis of the androgen regulated homeobox gene NKX3.1 in benign and malignant prostate epithelium. J Urol 2001;165:1329–34.
6. Bostwick DG, Qian J. High-grade prostatic intraepithelial neoplasia. Mod Pathol 2004;17:360–79.
7. Emmert-Buck MR, Vocke CD, Pozzatti RO, et al. Allelic loss on chromosome 8p12-21 in microdissected prostatic intraepithelial neoplasia. Cancer Res 1995;55:2959–62.

8. Haggman MJ, Wojno KJ, Pearsall CP, Macoska JA. Allelic loss of 8p sequences in prostatic intraepithelial neoplasia and carcinoma. Urology 1997;50:643–7.

9. Nelson WG, De Marzo AM, Deweese TL, et al. Preneoplastic prostate lesions: an opportunity for prostate cancer prevention. Ann N Y Acad Sci 2001; 952:135–44.

10. Bhatia-Gaur R, Donjacour AA, Sciavolino PJ, et al. Roles for Nkx3.1 in prostate development and cancer. Genes Dev 1999;13:966–77.

11. Schneider A, Brand T, Zweigerdt R, Arnold H. Targeted disruption of the Nkx3.1 gene in mice results in morphogenetic defects of minor salivary glands: parallels to glandular duct morphogenesis in prostate. Mech Dev 2000;95:163–74.

12. Tanaka M, Komuro I, Inagaki H, Jenkins NA, Copeland NG, Izumo S. Nkx3.1, a murine homolog of *Drosophila* bagpipe, regulates epithelial ductal branching and proliferation of the prostate and palatine glands. Dev Dyn 2000;219:248–60.

13. Kim MJ, Bhatia-Gaur R, Banach-Petrosky WA, et al. Nkx3.1 mutant mice recapitulate early stages of prostate carcinogenesis. Cancer Res 2002;62:2999–3004.

14. Kim MJ, Cardiff RD, Desai N, et al. Cooperativity of Nkx3.1 and Pten loss of function in a mouse model of prostate carcinogenesis. Proc Natl Acad Sci U S A 2002; 99:2884–9.

15. Abdulkadir SA, Magee JA, Peters TJ, et al. Conditional loss of Nkx3.1 in adult mice induces prostatic intraepithelial neoplasia. Mol Cell Biol 2002;22:1495–503.

16. Gao H, Ouyang X, Banach-Petrosky W, et al. A critical role for p27kip1 gene dosage in a mouse model of prostate carcinogenesis. Proc Natl Acad Sci U S A 2004; 101:17204–9.

17. Shen MM, Abate-Shen C. Roles of the Nkx3.1 homeobox gene in prostate organogenesis and carcinogenesis. Dev Dyn 2003;228:767–78.

18. Bowen C, Bubendorf L, Voeller HJ, et al. Loss of NKX3.1 expression in human prostate cancers correlates with tumor progression. Cancer Res 2000;60: 6111–5.

19. Korkmaz CG, Korkmaz KS, Manola J, et al. Analysis of androgen regulated homeobox gene NKX3.1 during prostate carcinogenesis. J Urol 2004;172:1134–9.

20. Asatiani E, Huang WX, Wang A, et al. Deletion, methylation, and expression of the NKX3.1 suppressor gene in primary human prostate cancer. Cancer Res 2005;65:1164–73.

21. Xu LL, Srikantan V, Sesterhenn IA, et al. Expression profile of an androgen regulated prostate specific homeobox gene NKX3.1 in primary prostate cancer. J Urol 2000;163:972–9.

22. De Marzo AM, Platz EA, Epstein JI, et al. A working group classification of focal prostate atrophy lesions. Am J Surg Pathol 2006;10:1281–91.

23. Franks LM. Atrophy and hyperplasia in the prostate proper. J Pathol Bacteriol 1954;68:617–21.

24. De Marzo AM, Marchi VL, Epstein JI, Nelson WG. Proliferative inflammatory atrophy of the prostate: implications for prostatic carcinogenesis. Am J Pathol 1999;155:1985–92.

25. Putzi MJ, De Marzo AM. Morphologic transitions between proliferative inflammatory atrophy and high-grade prostatic intraepithelial neoplasia. Urology 2000; 56:828–32.

26. Shah R, Mucci NR, Amin A, Macoska JA, Rubin MA. Postatrophic hyperplasia of the prostate gland: neoplastic precursor or innocent bystander? Am J Pathol 2001; 158:1767–73.

27. Nakayama M, Bennett CJ, Hicks JL, et al. Hypermethylation of the human GSTP1 CpG island is present in a subset of proliferative inflammatory atrophy lesions but not in normal or hyperplastic epithelium of the prostate: a detailed study using laser-capture microdissection. Am J Pathol 2003;163:923–33.

28. Liavag I. Atrophy and regeneration in the pathogenesis of prostatic carcinoma. Acta Pathol Microbiol Scand 1968;73:338–50.

29. Montironi R, Mazzucchelli R, Scarpelli M. Precancerous lesions and conditions of the prostate: from morphological and biological characterization to chemoprevention. Ann N Y Acad Sci 2002;963:169–84.

30. Ruska KM, Sauvageot J, Epstein JI. Histology and cellular kinetics of prostatic atrophy. Am J Surg Pathol 1998;22:1073–7.

31. Nelson WG, De Marzo AM, Isaacs WB. Prostate cancer. N Engl J Med 2003;349:366–81.

32. Nakayama M, Bennett CJ, Hicks JL, et al. Hypermethylation of the human glutathione *S*-transferase-π gene (GSTP1) CpG island is present in a subset of proliferative inflammatory atrophy lesions but not in normal or hyperplastic epithelium of the prostate: a detailed study using laser-capture microdissection. Am J Pathol 2003;163:923–33.

33. Parsons JK, Nelson CP, Gage WR, Nelson WG, Kensler TW, De Marzo AM. GSTA1 expression in normal, preneoplastic, and neoplastic human prostate tissue. Prostate 2001;49:30–7.

34. Zha S, Gage WR, Sauvageot J, et al. Cyclooxygenase-2 is up-regulated in proliferative inflammatory atrophy of the prostate, but not in prostate carcinoma. Cancer Res 2001;61:8617–23.

35. Knudsen BS, Lucas JM, Fazli L, et al. Regulation of hepatocyte activator inhibitor-1 expression by androgen and oncogenic transformation in the prostate. Am J Pathol 2005;167:255–66.

36. van Leenders GJ, Gage WR, Hicks JL, et al. Intermediate cells in human prostate epithelium are enriched in proliferative inflammatory atrophy. Am J Pathol 2003;162:1529–37.

37. Faith DA, Isaacs WB, Morgan JD, et al. Trefoil factor 3 overexpression in prostatic carcinoma: prognostic importance using tissue microarrays. Prostate 2004;61: 215–27.

38. Jenkins RB, Qian J, Lieber MM, Bostwick DG. Detection of c-myc oncogene amplification and chromosomal anomalies in metastatic prostatic carcinoma by fluorescence *in situ* hybridization. Cancer Res 1997; 57:524–31.

39. Applied Biosystems. Applied Biosystems online technical document: essentials of real time PCR. Foster City (CA): Applied Biosystems; 2003.

40. Magee JA, Abdulkadir SA, Milbrandt J. Haploinsufficiency at the Nkx3.1 locus. A paradigm for stochastic, dosage-sensitive gene regulation during tumor initiation. Cancer Cell 2003;3:273–83.

41. Macoska JA, Trybus TM, Wojno KJ. 8p22 loss concurrent with 8c gain is associated with poor outcome in prostate cancer. Urology 2000;55:776–82.

42. Matsuyama H, Pan Y, Yoshihiro S, et al. Clinical significance of chromosome 8p, 10q, and 16q deletions in prostate cancer. Prostate 2003;54:103–11.

43. Zhou W, Goodman M, Lyles RH, et al. Surgical margin and Gleason score as predictors of postoperative recurrence in prostate cancer with or without chromosome 8p allelic imbalance. Prostate 2004;61:81–91.

44. Ribeiro FR, Diep CB, Jeronimo C, et al. Statistical dissection of genetic pathways involved in prostate carcinogenesis. Genes Chromosomes Cancer 2006;45: 154–63.

45. Ouyang X, DeWeese TL, Nelson WG, Abate-Shen C. Loss-of-function of Nkx3.1 promotes increased oxidative damage in prostate carcinogenesis. Cancer Res 2005;65: 6773–9.

46. Li X, Guan B, Maghami S, Bieberich CJ. NKX3.1 is regulated by protein kinase CK2 in prostate tumor cells. Mol Cell Biol 2006;26:3008–17.

47. Chen H, Bieberich CJ. Structural and functional analysis of domains mediating interaction between NKX-3.1 and PDEF. J Cell Biochem 2005;94:168–77.